Calorimetric Measurement of Phospholipid Interaction with Methyl-β-Cyclodextrin†

Thomas G. Anderson,* Anmin Tan, Peter Ganz, and Joachim Seelig

Department of Biophysical Chemistry, Biozentrum of the University of Basel, Basel, Switzerland

Received October 21, 2003; Revised Manuscript Received January 8, 2004

ABSTRACT: Cyclodextrins are able to bind hydrophobic molecules in their interior cavity and as such have received a great deal of attention as carriers of cholesterol, lipophilic drugs, and other sparingly soluble compounds. Despite the importance of these biochemical applications, relatively little is known about the interactions of cyclodextrins with phospholipid membranes. Here we characterize the binding of randomly methylated β-cyclodextrin (mβCD) to 1-palmitoyl-2-oleoyl-*sn*-glycero-3-phosphocholine (POPC) using right-angle light scattering and isothermal titration calorimetry. Existing models of lipophile−membrane interactions are inadequate to describe the observed binding; we introduce a modified chemical reaction model in which the chemical activity of the phospholipid is independent of its concentration. We find that an average of four mβCD molecules bind to each POPC molecule with an enthalpy of reaction of 46 kJ mol^{-1} and an equilibrium constant of 90 M^{-3}. These results are consistent with earlier qualititative observations and suggest that disruption of phospholipid membranes may be minimized if the concentration of mβCD is kept below about 15 mM.

Cyclodextrins (CDs) are cyclic oligosaccharides formed by bacterial degradation of starch, and typically contain six (αCD), seven (βCD),[1] or eight (γCD) glucose residues linked by (1 → 4) glycosidic bonds (*1*). They feature a relatively nonpolar cylindrical cavity, which can bind and thereby solublize a wide variety of hydrophobic molecules (*2*). As such, they have attracted wide interest as potential agents for drug delivery (*3*) and cholesterol sequestration (*4*−*6*), among many other applications.

The interaction of cyclodextrins with cholesterol has been studied in detail in monolayer (*7*, *8*) and bilayer (*9*) membrane model systems, as well as with living cells (*10*, *11*) and molecular modeling studies (*12*). However, despite the demonstrated effectiveness of cyclodextrins in biomedical applications, relatively little is known about the interactions of these molecules with the nonsterol components of biological membranes. Most of what is known comes indirectly from studies of cyclodextrin and cholesterol. For example, Ohtani and co-workers showed in 1989 that native cyclodextrins promote the release of phospholipids from erythrocyte ghost membranes, in the order α > β ≫ γ, but do not themselves bind to the membranes (*13*). Other workers later showed that a randomly methylated derivative of the β form of CD (mβCD) could extract nonsterol components from skin stratum corneum (*14*) and retinal rod disk membranes (*15*). That the degree of lipid extraction is highly sensitive to the concentration of cyclodextrins was demonstrated by Ohvo and Slotte, who measured the rate of desorption of phospholipids from monolayers to βCD in the subphase (*7*), and Niu and Litman, who used membrane filtration to measure the amount of POPC extracted from bilayer vesicles by mβCD (*9*).

A few studies have been directed specifically at the interaction of cyclodextrins with phospholipids. Several groups have inferred extraction of dipalmitoylphosphatidylcholine (DPPC) from vesicles by αCD and dimethyl-βCD (but not other cyclodextrins) on the basis of differential scanning calorimetry (*16*, *17*). Others have measured the interaction of αCD with multilayers of phospholipids bearing different headgroups by nuclear magnetic resonance spectroscopy (*18*, *19*). In a particularly thorough study, Nishijo and co-workers used carboxyfluorescein leakage to monitor disruption of phospholipid vesicles by several substituted and unsubstituted cyclodextrins (*20*). In addition to these studies with natural phospholipids, Tanhuanpää and co-workers have used excimer fluorescence to examine the interaction of γ-cyclodextrins with pyrene-labeled phospholipids (*21*, *22*).

Interactions of lipophilic molecules with membranes are of great biological and pharmacological interest. Lipophiles

† Financial support from Swiss National Science Foundation Grant No. 31-58800.99 is acknowledged.

* To whom correspondence should be addressed. Mailing address: Klingelbergstrasse 70, CH4056 Basel, Switzerland. Tel: +41 61 267 21 92. Fax: +41 61 267 21 89. E-mail: thomas.anderson@unibas.ch.

[1] Abbreviations: a_L, chemical activity of lipid; βCD, β-cyclodextrin; c_L, concentration of free (uncomplexed) lipid; c_L^0, total lipid concentration; c_D, concentration of free (uncomplexed) cyclodextrin; c_D^0, total cyclodextrin concentration; c_Φ, concentration of lipid−cyclodextrin inclusion complex; cbc, critical bilayer concentration; D, cyclodextrin molecule; DSC, differential scanning calorimetry; ΔH_Φ°, heat of formation of lipid−cyclodextrin inclusion complex; ΔH_1°, heat of formation of a 1:1 lipid−cyclodextrin inclusion complex; ΔH_i°, heat of reaction for addition of a cyclodextrin molecule to an inclusion complex; ITC, isothermal titration calorimetry; K_Φ, equilibrium constant for formation of a lipid−cyclodextrin inclusion complex; K_1, equilibrium constant for formation of a 1:1 lipid−cyclodextrin inclusion complex; K_i, equilibrium constant for addition of a cyclodextrin molecule to an inclusion complex; L, lipid molecule; L_b, lipid molecule in the bilayer phase; L_{aq}, lipid molecule in the aqueous phase; LUV, large unilamellar vesicle; mβCD, randomly methylated βCD; MLV, multilamellar vesicle; POPC, 1-palmitoyl-2-oleoyl-*sn*-glycero-3-phosphocholine; $\bar{Q}_{inj}$, heat of injection per mole of injectant; SUV, small unilamellar vesicle; V_{cell}, volume of the calorimeter cell; ΔV_{inj}, injection volume; ν, stoichiometry of a lipid−cyclodextrin inclusion complex; Φ, lipid−cyclodextrin inclusion complex; Φ_ν, lipid−cyclodextrin inclusion complex with 1:ν stoichiometry.

10.1021/bi0358869 CCC: $27.50
Published on Web 02/06/2004

tend to partition strongly into lipid membranes or form micellar structures into which the lipid can partition or both. This binding has been successfully described in terms of the bulk concentrations of the lipophile and lipid components (*23*), although there has been some disagreement as to the most appropriate way to express the equilibrium conditions. Cyclodextrins, in contrast, do not form micelles and appear not to bind to lipid membranes (*13*, *17*); rather, they extract lipid components to form inclusion complexes of discrete composition (*17*). As a result, existing models of lipophile/membrane interactions do not apply. On the other hand, it is also not appropriate to describe the lipid vesicles as an aqueous solution, so the classical solution-phase A + B $\rightleftarrows$ A·B model (*24*) is not adequate either. It is therefore necessary to introduce a new thermodynamic model that combines elements of both approaches.

Our aim in the present study is to characterize the interaction of one phospholipid, 1-palmitoyl-2-oleoyl-*sn*-glycero-3-phosphatidylcholine (POPC), with randomly methylated β-cyclodextrin (mβCD). This particular cyclodextrin derivative is widely used because of its greatly enhanced solubility compared with natural β-cyclodextrin (*3*). POPC was chosen for these studies because it has been thoroughly characterized calorimetrically and has a low P_β to L_α transition temperature ($T_c = -5$ °C); we therefore avoid potential complications arising from this transition. Along with measurements of right-angle light scattering, we use the technique of isothermal titration calorimetry (ITC), which is able to provide detailed thermodynamic information about an intermolecular interaction, principally the binding constant K_b and enthalpy of binding ΔH_b (*24*).

MATERIALS AND METHODS

Materials. 1-Palmitoyl-2-oleoyl-*sn*-glycero-3-phosphocholine (POPC) was obtained from Avanti Polar Lipids (Alabaster, AL). Methyl-β-cyclodextrin (mβCD) was purchased from Fluka (Buchs, Switzerland). All other chemicals were of analytical or reagent grade. Buffer (10 mM tris(hydroxymethyl)aminomethane, 100 mM NaCl, pH 7.4) was prepared from 18 MΩ water obtained from a NANOpure A filtration system.

Preparation of Vesicles. A defined amount of lipid in chloroform was dried under nitrogen and weighed by difference. The lipid was twice dissolved in dichloromethane and dried under nitrogen and, subsequently, overnight under high vacuum. Typically, 2−3 mL of buffer was added to the lipid, and the dispersion was vortexed vigorously. Small unilamellar vesicles (SUVs) with an average diameter of 30 nm were prepared by sonication in ice water using a titanium-tip ultrasonicator (10−15 min) until the solution became transparent. Titanium debris from the tip of the ultrasonicator probe was removed by centrifugation (Eppendorf tabletop centrifuge, 4 min at $(1.6 \times 10^4)g$). Large unilamellar vesicles (LUVs) with diameters of 50 or 100 nm were prepared by extrusion using polycarbonate filters with 50- or 100-nm pore size, respectively (*25*). Multilamellar vesicles (MLVs) were prepared by three freeze/thaw cycles of the lipid suspension.

Right-Angle Light Scattering. Light-scattering measurements were made with a Jasco FP 777 spectrofluorimeter (Japan-Spectroscopic, Tokyo, Japan) with the excitation wavelength set at 350 nm. The optical cuvette with 3 mL of the cyclodextrin solution at room temperature (~23 °C) was continuously stirred. Vesicles (30-nm diameter) were added in 5−50 μL aliquots using a Hamilton syringe. The scattering intensity at 350 nm was recorded as a function of time. In a control measurement, vesicles were injected into buffer without cyclodextrin.

Calorimetry. Isothermal titration calorimetry was performed at a temperature of 28 °C using MicroCal Omega and VP high-sensitivity titration calorimeters (MicroCal, Northampton, MA) (*24*). To avoid air bubbles, all solutions were degassed under vacuum prior to use. The data were acquired by computer software developed by MicroCal and analyzed with a custom-designed program using Mathematica (Wolfram Research, Champaign, IL). During a titration experiment, the heat measured for the first injection is usually a few percent low because of diffusive mixing in the syringe tip during baseline acquisition and other factors. To minimize the impact of this error, a minimal volume of 1 μL was always used for the first injection, and the accompanying heat was omitted from the data analysis.

Dilution of mβCD during the course of a titration is highly exothermic. To correct for this effect, the heat of dilution was measured in a separate titration of buffer into mβCD solution. The resulting heat values were subtracted from the corresponding experimental measurements.

Binding Model. Historically, the interactions between molecules in ITC experiments have been modeled either as a solution-phase complexation reaction, A(aq) + B(aq) $\rightleftarrows$ A·B(aq) (*24*), or as a partitioning between a bilayer and a solution or micelles or both (*23*). In the case of interactions between lipophilic molecules and lipid bilayers, the partition model has been widely used with good results. However, cyclodextrins do not seem to penetrate into phospholipid bilayers (*13*, *17*), so the partitioning model is not useful in the present study. On the other hand, our results are not consistent with the classical complexation model either (see results). For the present study, we have developed a different binding model, which incorporates elements of both the complexation and partitioning models.

The binding of POPC to mβCD is modeled by the chemical equation

$$L_b + \nu D \rightleftarrows \Phi \tag{1}$$

where L_b represents a lipid molecule in the bilayer pseudophase, D is the mβCD molecule, and Φ represents the inclusion complex $L{\cdot}D_\nu$, which comprises one lipid and ν cyclodextrin molecules. Except where indicated otherwise, we make the simplifying assumption that every inclusion complex has the same 1:ν stoichiometry; whenever there may be ambiguity, we denote a complex with one lipid and j cyclodextrin molecules as Φ_j. The molar heat of inclusion complex formation is $\Delta\bar{H}^\circ_\Phi$ and the equilibrium constant is K_Φ.

By the law of mass action, the total concentrations of lipid and cyclodextrin are, respectively,

$$c_L^0 = c_{L_b} + c_{L(aq)} + c_\Phi \tag{2}$$

and

$$c_D^0 = c_D + \nu c_\Phi \tag{3}$$

Here L(aq) refers to monomers of lipid present in the aqueous phase at a very low concentration. For POPC, the maximum solubility of the lipid monomers (the "critical bilayer concentration" or cbc) is estimated to be less than 10^{-9} M (*26*); for the purposes of this study, we treat this value as equal to zero.

The equilibrium binding constant is defined in terms of the chemical activities of the species involved in the reaction, $K_\Phi \equiv a_\Phi/[a_L(a_D)^\nu]$. Following convention, we set the activities of mβCD and the inclusion complex equal to their respective molar concentration in solution. The activity of POPC molecules in the vesicle pseudophase is less well-defined. In the lipid partition model, the activity of a lipid is set equal to its bulk concentration in solution (*23*) or to its mole fraction in the membrane (*27*). To the extent that the chemical environment of L_b is dominated by the phospholipid bilayer, a_L is independent of the lipid concentration, although it may vary with the size of the vesicles. We choose the vesicle pseudophase as the standard state for POPC, so $a_L \equiv 1$, regardless of concentration and vesicle size. This is similar to the mole-fraction formulation of the partition model, except in our model the mole fraction of lipid in the bilayer is always equal to 1.

With these definitions, the expression for the equilibrium constant for reaction 1 is

$$K_\Phi = \frac{c_\Phi}{(a_L)(c_D)^\nu} \tag{4}$$

When POPC vesicles are present in any amount in the cell, the activity of the lipid is unity, and it is straightforward to evaluate this expression. If all of the vesicles are dissolved, however, the activity of the lipid is less than 1. In this case, the activity of the lipid can be expressed in terms of the equilibrium constant K_Φ using the mass-action equations 2 and 3 with c_{L_b} and $c_{L(aq)}$ equal to zero. This gives as an overall expression for the chemical activity of the lipid

$$a_L = \begin{cases} 1 & \text{(vesicles)} \\ \dfrac{c_L^0}{K_\Phi(c_D^0 - \nu c_L^0)^\nu} & \text{(no vesicles)} \end{cases} \tag{5}$$

Equation 5 holds as long as the concentration of lipid monomers in solution is much less than the total concentration of lipid. Since the estimated cbc of POPC is several orders of magnitude lower than the lipid concentrations used in this study, this is a reasonable approximation.

This expression for the activity of the lipid can be derived more rigorously on the basis of the ratio of the actual concentration of aqueous lipid monomers to the cbc. When vesicles are present, $c_{L(aq)}$ = cbc, giving an activity of 1. When all of the lipid is dissolved, the ratio $c_{L(aq)}$/cbc is less than or equal to 1. This is equivalent to eq 5 in the limit of cbc $\rightarrow$ 0. This result means that *it is not necessary for us to know the precise value of the cbc*, only that it is very low.

The concentration of the inclusion complex Φ in the cell, like the chemical activity of the lipid, is a piecewise function of the overall composition. As indicated above, when the lipid is fully dissolved, $c_\Phi \doteq c_L^0$. When vesicles are present in coexistence with the complexes, the activity of the lipid is 1, and from eq (4), $c_\Phi = K_\Phi(c_D)^\nu$. In conjunction with the mass-action equation 3, this gives $c_\Phi = K_\Phi(c_D^0 - \nu c_\Phi)^\nu$, which has no simple analytical solution for values of ν greater than 2. The boundary condition between these two cases, which corresponds to the point at which vesicles just begin to coexist with complex, is defined by equality of the two branches of eq 5,

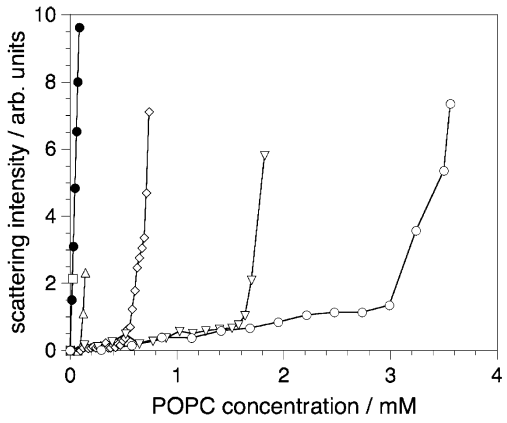

FIGURE 1: Ninety degree light scattering intensity as a function of phospholipid concentration as phospholipid vesicles are titrated into buffer or solutions of different cyclodextrin concentration. POPC SUVs (30 nm) were titrated into buffer (●) or mβCD solutions at concentrations of 20 (□), 40 (△), 60 (◇), 80 (▽), and 100 mM (○) at room temperature (~23 °C).

$$\frac{c_L^0}{K_\Phi(c_D^0 - \nu c_L^0)^\nu} = 1 \qquad \text{(boundary)} \tag{6}$$

If we designate the left-hand side of eq 6 as *f*, then the overall expression for the concentration of the inclusion complex is defined implicitly by

$$c_\Phi = \begin{cases} c_L^0 & (f \le 1) \\ K_\Phi(c_D^0 - \nu c_\Phi)^\nu & (f > 1) \end{cases} \tag{7}$$

During a titration, POPC vesicles are mixed with mβCD in the calorimeter cell. The heat associated with formation of inclusion complexes is

$$dQ = \Delta\bar{H}_\Phi^\circ \, dn_\Phi \tag{8}$$

This heat, along with the heat of dilution of the mβCD and the lipid, is measured during the ITC experiment. The amount of complex in the cell is $n_\Phi = V_{cell}c_\Phi$.

The binding model presented here is strictly thermodynamic in nature and does not address the question of the mechanism of mβCD binding to POPC. Other aspects of this study, however, do provide some mechanistic insight (see Discussion).

RESULTS

Dissolution of POPC Vesicles by mβCD. Measurement of the intensity of right-angle light scattering showed that POPC vesicles dissolve when introduced into a solution of mβCD (Figure 1). In this experiment, aliquots of POPC vesicles were injected into a spectrofluorimeter cell that contained buffer with or without mβCD. In the absence of mβCD, the intensity of light scattering increased as a linear function of the concentration of POPC in the cell. When mβCD was present in the cell at sufficiently high concentra-

tion, the scattering intensity increased much more gradually with POPC concentration. This suggests that the relatively large injected vesicles, which strongly scatter light, were dissolving to form much smaller structures. As more vesicles were added to the cell, eventually they ceased to dissolve, and further addition of POPC caused the scattering intensity to increase much more rapidly, albeit with a somewhat lower slope than that observed for injection of vesicles into pure buffer. The extent of vesicle dissolution varied strongly with the concentration of mβCD in the cell: a 25% increase in mβCD concentration from 80 to 100 nM led to a 2-fold increase in the amount of POPC that dissolved in the solution (Figure 1, inverted triangles vs open circles).

The interaction of mβCD with POPC was measured in greater detail by isothermal titration calorimetry (Figures 2 and 3). When buffer is injected into mβCD solution, the resulting modest dilution is highly exothermic (Figure 2B). When POPC vesicles (0.25−40 mM) are injected into a mβCD solution (15−150 mM), the sharp dilution peaks are partially masked by much broader endothermic peaks (Figure 2A). The endothermic component of the peaks broadens during the course of the titration before eventually disappearing into the baseline; this is seen clearly in Figure 2C, which shows the difference between the raw data in parts A and B. We attribute this change in dissolution kinetics to the dilution of mβCD in the cell by about 20% over the course of the titration, although the degree of broadening suggests that additional factors may be involved.

The total heat of an injection is equal to the area between the titration peak and the baseline. Integrated heat values were determined separately for {POPC → mβCD} titrations and for the corresponding {buffer → mβCD} dilution controls. Taking the difference of these values gives the net heat for each injection (Figure 3). The titration curves for POPC injected into mβCD have a characteristic shape, comprising a nearly flat plateau of positive heat followed by a rapid drop toward zero; this is in marked contrast to a typical sigmoidal titration curve. The plateau part of the curve corresponds closely to the range of concentrations at which dissolution of POPC vesicles was observed by light scattering. The ratio of POPC to mβCD at the edge of the plateau varied strongly with the concentration of mβCD in the cell but in all cases was much less than 1. As such, the edge of the plateau does not correspond to a classical titration equivalence point, which would occur at a constant concentration ratio.

Within experimental error, the same results were obtained in a control titration in which the buffer was replaced by pure water (not shown). This rules out ionic strength and pH as significant contributors to the observed phenomena.

Heat of Inclusion Complex Formation. On the basis of our hypothesis that the plateau region of the titration curve corresponds to complete dissolution of injected POPC vesicles and formation of inclusion complexes between individual POPC molecules and mβCD, the heat per mole of POPC injected in this part of the titration is equal to $\Delta\bar{H}^{\circ}_{\Phi}$, the heat of formation of the inclusion complex. This result follows from eq 8 under the assumption that the concentration of free POPC monomers in solution is negligible.

The heat of inclusion complex formation was determined for four sizes of POPC vesicle: small unilamellar vesicles

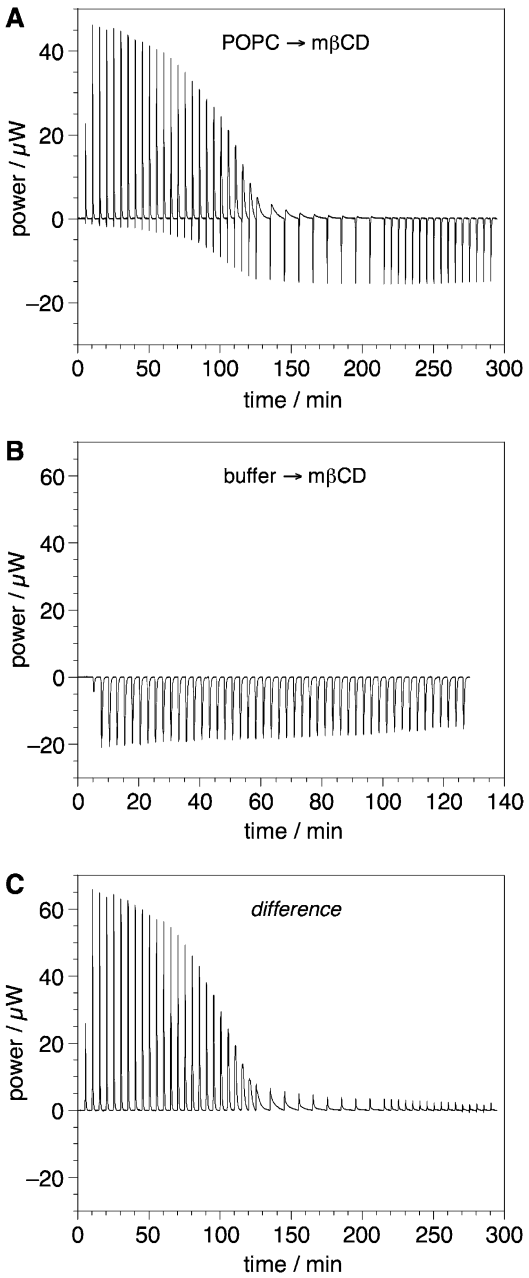

FIGURE 2: Titration of phospholipid into cyclodextrin. Panel A presents titration of 50-nm unilamellar POPC vesicles (7.77 mM) into mβCD (60 mM) in buffer at 28 °C. Each peak corresponds to the injection of 5 μL of vesicle suspension into the mβCD solution in the calorimeter cell (cell volume = 1.4037 mL), except the first peak, in which 1 μL was injected (see text). Panel B presents control measurement in which buffer was injected into the same mβCD solution as in that in panel A. Panel C presents the difference between the curves in panels A and B.

(SUVs) of 30 nm diameter prepared by sonication and of 50 and 100 nm diameter prepared by extrusion, and multilamellar vesicles (MLVs) prepared by repeated freeze/thaw cycles. In the case of the MLV titrations, dissolution of injected vesicles proceeded much more slowly than for the SUVs, and there was a greater amount of baseline noise. Nevertheless the amount of heat was large enough to be measured with fair precision. In all cases, the shape of the titration curve was broadly similar. The best-fit value of $\Delta\bar{H}^{\circ}_{\Phi}$ decreased from 46 ± 14 kJ mol^{-1} for 30 nm vesicles (N = 10) to 40 ± 8 kJ mol^{-1} for 50 nm vesicles (N = 3)

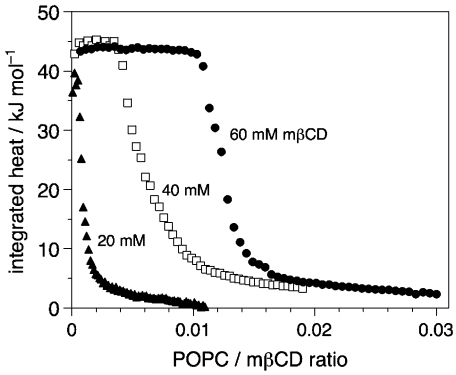

FIGURE 3: Corrected heat of reaction per mole of POPC injected as a function of the ratio of POPC to mβCD in the calorimeter cell for titrations of 50-nm unilamellar POPC vesicles into mβCD with an initial cell concentration of 20 (▲), 40 (□), and 60 mM (●). For these titrations, the concentration of POPC in the syringe was 1, 5, and 7.77 mM, respectively.

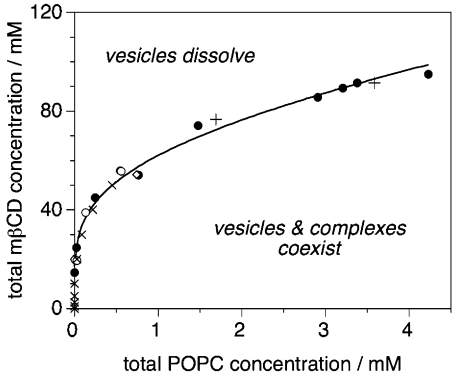

FIGURE 4: Phase diagram of POPC−mβCD at 28 °C showing the solubilization phase boundary between the inclusion complex phase and the region of inclusion complex/vesicle coexistence for SUVs (●), LUVs (○), and MLVs (◇). The solid line was obtained from eq 9 using a stoichiometric coefficient of $\nu = 4$ and an equilibrium constant of $K_\Phi = 90$ M^{-3}. The + symbols show the break points of the light-scattering measurements (Figure 1). The × symbols indicate solubility values based on the results reported by Niu and Litman (*9*).

and 33 ± 8 kJ mol^{-1} for 100 nm vesicles ($N = 3$); a value of 46 ± 7 kJ mol^{-1} was obtained for the multilamellar vesicles ($N = 2$). Because of the large uncertainty of the measured values, the differences among them cannot be judged to be significant.

As a check on the value of $\Delta\bar{H}^\circ_\Phi$, a sample of POPC/mβCD inclusion complexes was prepared prior to titration by suspending a film of POPC in a solution of mβCD with a final composition of 6 mM POPC and 120 mM mβCD. As expected on the basis of the results described above, the POPC rapidly dissolved upon vortexing at room temperature. When an aliquot of this solution was titrated into buffer, the net heat of injection was found to be −40 ± 1.3 kJ per mole of POPC injected (not shown). This is in good agreement with the other titration data and is consistent with complete dissociation of the inclusion complexes and formation of POPC vesicles upon injection. This is the reverse of the situation in the earlier titrations; hence the negative sign. The net heat of injection was constant for the first five injections of 7 μL aliquots, after which its magnitude decreased; the reasons for this are not yet clear.

The binding of POPC to natural β-cyclodextrin (βCD) and to 2-hydroxypropyl-β-cyclodextrin (hpβCD) were also measured (not shown). Unlike the randomly methylated form, βCD has a small heat of dilution, which is endothermic rather than exothermic, and its solublility in water is very low (∼16 mM (*28*)). It was found that enthalpy of interaction of POPC vesicles with βCD was negative, but the low concentrations required in the titrations prevented us from measuring the heat of binding or the equilibrium constant. No detectable interaction was observed in titrations of POPC into hpβCD, but there is some evidence that hpβCD can dissolve POPC vesicles on a time scale of hours to days.

Extent of POPC Solubilization by mβCD. Figure 3 shows that the extent of the plateau region of the titration curve varies strongly with the concentration of mβCD in the cell. Taking this plateau region as a proxy for the range of concentrations at which POPC completely dissolves in mβCD solution, we can estimate the extent of POPC solubility from the composition at the breakpoint in the titration curve. The compositions at these points for the titrations performed in this study lie along a smooth curve, as shown in Figure 4. At compositions that lie above this curve, the calorimeter cell contains an aqueous solution of POPC−mβCD inclusion complexes, free mβCD, and perhaps a very small amount of aqueous POPC monomers. Below the curve, intact vesicles coexist with the aqueous inclusion complexes. The *x*-intercept of the solubility curve corresponds to the cbc, the concentration of POPC that dissolves in water in the absence of cyclodextrin. As noted above, we have taken this value to be zero.

The inclusion complexes of mβCD and POPC are assumed to all have the same stoichiometry; the validity of this assumption is addressed in the Discussion. The boundary curve of the region of POPC vesicle/inclusion complex coexistence corresponds to eq 6. This equation is easily solved to give the boundary equation

$$c_D^0 = \nu c_L^0 + \left(\frac{c_L^0}{K_\Phi}\right)^{1/\nu} \qquad (9)$$

A least-squares fit of eq 9 to the measured boundary points gives $\nu = 4.3 \pm 0.2$ and $K_\Phi = 210 \pm 140$ M$^{-3.3}$. The large uncertainty and unusual units for the equilibrium constant arise from a tight coupling between the values of K_Φ and ν. If the inclusion complex stoichiometry is fixed at the integer value of $\nu = 4$, the best-fit equilibrium constant becomes $K_\Phi = 90 \pm 5$ M^{-3}. This fit is shown by the solid line in Figure 4.

For comparison, Figure 4 also shows the compositions at the break points of the light-scattering measurements discussed above (+), as well as values based on measurements of POPC extraction by mβCD (×) reported by Niu and Litman (*9*). These points are in excellent agreement with the results of our ITC measurements.

Titration of mβCD into POPC vesicles. A small number of "reverse" titrations were performed in which a mβCD solution was injected into a suspension of POPC vesicles; the net heats of injection are plotted in Figure 5. The raw titration data resembled the dilution control shown in Figure 2B and are not shown. The composition of the cell remained well within the range of vesicle/inclusion complex coexistence throughout the titrations, so the extent of vesicle dissolution was small. Accordingly, the measured heats of

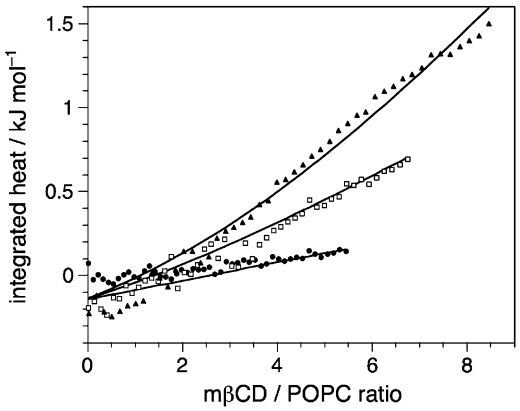

FIGURE 5: Titration of mβCD into a suspension of POPC vesicles in buffer. The concentrations used were 50 mM mβCD into 2.51 mM POPC (●), 100 mM mβCD into 4.055 mM POPC (□), and 150 mM mβCD into 4.85 mM POPC (▲). The solid lines are fits to the data using a stepwise complex formation model (see text.).

injection were very similar to those of the control titrations of mβCD into buffer. The measurements plotted in Figure 5 therefore represent the difference between two large values, which accounts for the pronounced scatter in the data.

Based on the values obtained for K_Φ and $\Delta\bar{H}^\circ_\Phi$, the amount of the inclusion complex L·D$_4$ (Φ_4) that is expected to be formed during these titrations is far too small to account for the measured net heats of injection. In the "forward" titrations of POPC into mβCD described above, the Φ_4 inclusion complex is expected to be formed almost exclusively (see Discussion). However, this need not be the case in the reverse titrations. There the concentration of mβCD in the cell is roughly an order of magnitude lower than that in the forward titrations. With less mβCD in the cell, the equilibrium should favor complexes containing fewer mβCD molecules. To test this idea, we fit the data in Figure 5 to a mechanism of stepwise complex formation,

$$\begin{aligned} L_b + D &\rightleftarrows \Phi_1 \\ \Phi_1 + D &\rightleftarrows \Phi_2 \\ \Phi_2 + D &\rightleftarrows \Phi_3 \\ \Phi_3 + D &\rightleftarrows \Phi_4 \end{aligned} \tag{10}$$

This mechanism involves the formation of an initial inclusion complex between bilayer-phase POPC and a single mβCD molecule, followed by incremental attachment of three more mβCD molecules. Each of these steps has its own heat of reaction and equilibrium constant, for a total of eight parameters. Note that the first step involves removal of a phospholipid molecule from the bilayer environment into the aqueous phase prior to, or simultaneous with, binding to a cyclodextrin; the other three steps only involve binding of a cyclodextrin to the nascent complex. Since the exposure of a hydrophobic molecule to water tends to be exothermic (*29*), we expect the enthalpy change of the first step to be significantly lower (more negative) than those for the other steps.

The complete model (eq 10) has so many adjustable parameters that any fit to the experimental data would be unreliable. To reduce the number of fitting parameters to a more manageable level, we made some simplifying assumptions. Since the hydrophobic surface of the phospholipid's acyl chains is large compared to the size of the mβCD cavity (see Discussion), all four of the steps in eq 10 are likely to involve sequestration of a similar amount of hydrophobic surface. As an approximation, we take the energetics of this sequestration to be the same for each of the four steps. As noted above, the first step also involves the transfer of a phospholipid molecule out of the bilayer into an aqueous environment, so we assume that the first reaction will have very different overall energetics from the other three. In this way, we reduce our model parameters to four: $\Delta\bar{H}^\circ_1$ and K_1 for the first step and

$$\Delta\bar{H}^\circ_i \equiv \Delta\bar{H}^\circ_2 \doteq \Delta\bar{H}^\circ_3 \doteq \Delta\bar{H}^\circ_4 \tag{11}$$

and

$$K_i \equiv K_2 \doteq K_3 \doteq K_4 \tag{12}$$

for each of the remaining steps.

The overall combination of the steps in eq 10 is equivalent to the overall reaction described by eq 1 with $\nu = 4$. Therefore, the parameters here are further constrained by the observed heat of reaction and equilibrium constant of the overall reaction:

$$\Delta\bar{H}^\circ_\Phi = \Delta\bar{H}^\circ_1 + 3\Delta\bar{H}^\circ_i \tag{13}$$

and

$$K_\Phi = K_1 K_i^3 \tag{14}$$

With these constraints, we have reduced the number of adjustable fitting parameters to two, $\Delta\bar{H}^\circ_i$ and K_i. Finally, we made the simplifying assumption that the amount of each inclusion complex formed was very small compared to the total amount of cyclodextrin in the cell. Then $c_D \doteq c^0_D$ and from eq 4,

$$c_{\Phi_\nu} \doteq K_1 K_i^{\nu-1} (c^0_D)^\nu = K_\Phi K_i^{\nu-4} (c^0_D)^\nu \tag{15}$$

The net heat of injection for the reverse titration contains the sum of contributions from each of the steps in eq 10. Using eq 8, this gives

$$dQ \doteq \sum_{\nu=1}^{4} (\Delta\bar{H}^\circ_\Phi + (\nu-4)\Delta\bar{H}^\circ_i) V_{cell} K_\Phi K_i^{\nu-4} \nu (c^0_D)^{\nu-1}\, dc^0_D \tag{16}$$

The measured net heats of injection for the three reverse titrations were simultaneously fit to the expression in eq 16; the result is shown by the solid lines in Figure 5. The best-fit values obtained for the incremental reaction parameters are $\Delta\bar{H}^\circ_i = 14.86 \pm 0.05$ kJ mol^{-1} and $K_i = 10.4 \pm 0.3$ M^{-1}. The corresponding values for the first reaction step are $\Delta\bar{H}^\circ_1 = -1.8 \pm 0.1$ kJ mol^{-1} and $K_1 = 0.081 \pm 0.006$ (this equilibrium constant is dimensionless). As expected, $\Delta\bar{H}^\circ_1$ is much lower than $\Delta\bar{H}^\circ_i$. Despite the apparent precision of the least-squares fit, these values should be regarded as first approximations in light of the assumptions involved. Nevertheless they give an idea of the magnitude of these thermodynamic parameters.

Temperature Dependence. To examine the temperature dependence of cyclodextrin-mediated disruption of POPC

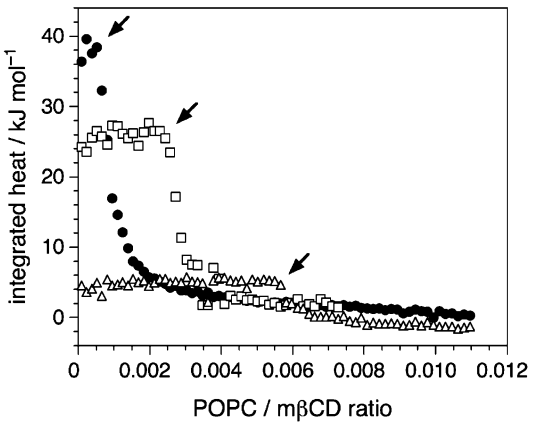

FIGURE 6: Net heat of injection for titration of 50-nm unilamellar POPC vesicles (1 mM) into mβCD (20 mM) at 28 (●), 40 (□) and 60 °C (△). Arrows mark the solubilization boundary for each titration curve.

vesicles, a representative titration was repeated at temperatures of 28, 40, and 60 °C (Figure 6). The enthalpy of inclusion complex formation decreased as the temperature was raised from ~40 kJ mol^{-1} at 28 °C to ~4 kJ mol^{-1} at 60 °C. From this, we calculate a heat capacity change of $\Delta C_P^\circ = -1.0$ kJ mol^{-1} for the complexation reaction. The equilibrium constant, as determined from eq 9 with ν fixed at 4, increased from ~70 M^{-3} to ~1100 M^{-3} over the temperature range; we emphasize that these are approximate values based on an assumption of a constant stoichiometry for the inclusion complex.

DISCUSSION

Comparison with Detergent Solubilization of Lipid Vesicles. It is well-known that detergents such as sodium dodecyl sulfate (SDS) can solubilize phospholipids by partitioning into the lipid bilayer and subsequently dispersing the bilayer into detergent-rich aqueous micelles (*23*, *30*, *31*, *33*). Detergent-induced vesicle dissolution is qualitatively similar to the cyclodextrin-induced dissolution process reported here, but there are clear differences between the two. Vesicle dissolution by detergents is a gradual process in that detergents can dissolve in phospholipid bilayers, and phospholipids can dissolve in detergent micelles. As a result, titrations of vesicles into detergent involve a change from micelles to bilayers with an intermediate state of micelle/bilayer coexistence (*23*, *31*).

Cyclodextrins, on the other hand, do not appear to form micelles or partition into phospholipid bilayers. Calorimetric titrations of phospholipid into cyclodextrin solutions consequently show much more abrupt transitions than similar titrations into detergents. Measurements of right-angle light scattering are similar for the two types of titrations, although they differ in the details.

Shape of the Titration Curve. The technique of isothermal titration calorimetry was developed to study ligands binding to macromolecular hosts in aqueous solution. Because the concentrations of both ligand and host vary smoothly during the course of the experiment, the titration curve has a characteristic sigmoidal shape (Figure 7, solid line) with a midpoint that is very close to the equivalence point of the reaction and a steepness that correlates with the magnitude of the binding constant and the cooperativity of the reaction

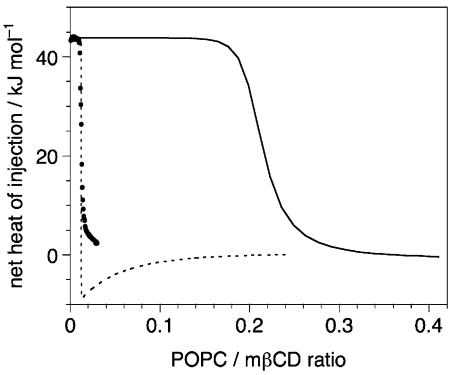

FIGURE 7: Calculated titration curves for the reaction L + 4D ⇄ Φ, using the concentrations of POPC and mβCD from Figure 2A. The solid line corresponds to a conventional titration in which all species are present in aqueous solution; the dotted line corresponds to the model described in the text, in which the injected POPC is initially in vesicle form. The corresponding experimental data are shown by filled circles. Values of $\Delta H_\Phi^\circ = 43$ kJ mol^{-1} and $K_\Phi = 90$ M^{-3} were used for both calculations.

(*24*). For such titrations, it is straightforward to fit the data to a binding model and obtain the stoichiometry, cooperativity, enthalpy, and equilibrium constant of the reaction.

More generally, a sigmoidal titration curve is expected whenever the chemical activities of the ligand and host species both change gradually with the composition of the mixture in the calorimeter cell. For example, many detergents can partition into lipid vesicle bilayers up to some limiting amount; likewise, individual lipid molecules can partition into the detergent micelles. In these cases, the compositions of the vesicles or micelles or both change smoothly during a titration and a smooth titration curve results that can be readily fit to an appropriate binding model (reviewed in ref *31*). Another example is demicellization of bile salts, for which the titration curves are sometimes highly asymmetric but nevertheless vary smoothly on either side of a critical micelle concentration (*32*).

The titration curves presented here for POPC vesicles injected into aqueous solutions of mβCD have a distinctly different shape. These curves are highly asymmetric, with a flat "plateau" at the beginning followed by a sharp break and a steep drop toward zero net heat per injection (Figure 7, black dots). This drop does not correspond to an equivalence point: the ratio of POPC to mβCD at this point is not fixed, but instead depends in a sensitive way on the initial concentration of mβCD in the cell (Figure 3).

Plateau-shaped titration curves have been observed before in titrations of lipid vesicles into some detergents (*31*). In these cases, the plateau has been attributed to strong partitioning of the detergent into the vesicle bilayer, as follows. At the beginning of the titration, the injected vesicles rapidly become saturated with detergent and disintegrate into micelles. Because the same thing happens after each injection, the associated injection heats are uniform. Eventually, the detergent in the cell is depleted and is no longer sufficient to disintegrate the injected vesicles. At this point, the injection heat drops rapidly to zero (*31*). This picture does not seem to fit the POPC/mβCD titration curves, however. In the measurements presented here, the break points in the titration curves occur in the range of 100−1000 cyclodextrin molecules per phospholipid. It is unlikely that intact POPC vesicles could accommodate so much mβCD. Some parti-

tioning may occur, but this cannot be the source of the sharp breaks in the titration curves.

A titration curve with a plateau followed by a sharp break is a natural feature of the thermodynamic model introduced in this study. In this model, the net heat of an injection arises entirely from complex formation. Expressed per mole of injected lipid, this heat is (for small injection volumes) $\bar{Q}_{inj} = \Delta\bar{H}^{\circ}_{\Phi}\,(dn_{\Phi}/dn_{L})$ (see eq 8). In the first part of a titration of lipid into cyclodextrin, when all of the injected lipid dissolves to form inclusion complexes with cyclodextrin, $(dn_{\Phi}/dn_{L}) = 1$ and the molar net heat of injection is constant,

$$\bar{Q}_{inj} = \Delta\bar{H}^{\circ}_{\Phi} \qquad \text{(plateau)} \qquad (17)$$

The position of the break in the titration curve is given by eq 6; this is the point at which injected vesicles cease to dissolve and coexist with inclusion complexes and free cyclodextrin molecules in solution. Beyond the break, then, the concentration of lipid vesicles increases and the concentrations of inclusion complex and free cyclodextrin remain nearly constant. Hence, the net heat of injection drops to zero.

In fact, our binding model predicts that the net heat of injection should change sign, moving beyond zero and then slowly decaying to the baseline (Figure 7, dotted line). This occurs because as additional lipid is injected the inclusion complexes and cyclodextrin in the cell gradually become more dilute. Since lipid vesicles are present in the cell in this part of the titration, the chemical activity of the lipid is constant and the equilibrium concentration of inclusion complex is determined entirely by the concentration of free cyclodextrin. Therefore, dilution of the cyclodextrin drives the reaction (eq 1) *in reverse* with the result that the net heat of injection changes sign. The predicted magnitude of this heat can be calculated as follows. The concentration of complex is given implicitly by the equation $c_{\Phi} = K_{\Phi}(c^{0}_{D} - \nu c_{\Phi})^{\nu}$ (see eq 7). We can find an expression for the derivative (dn_{Φ}/dn_{L}) by differentiating both sides of this equation with respect to n_{L}, the total amount of injected lipid, and making the replacement $c_{\Phi} = n_{\Phi}/V_{cell}$. After some simplification, this gives a molar net heat of injection of

$$\bar{Q}_{inj} = \Delta\bar{H}^{\circ}_{\Phi} V_{cell}\left(\frac{\nu c_{\Phi}}{c^{0}_{D} + \nu(\nu - 1)c_{\Phi}}\right)\left(\frac{dc^{0}_{D}}{dn_{L}}\right) \qquad \text{(after break)} \qquad (18)$$

The first term in parentheses is positive and the derivative term is negative during this part of the titration. Further details about the calculation of the predicted titration curve are presented in the Appendix.

The calculated titration curve shown by the dotted line in Figure 7 was constructed using the best-fit values of $\Delta\bar{H}^{\circ}_{\Phi}$ and K_{Φ}. This calculation is in excellent agreement with the observed titration curve shown by the black dots, except that the observed curve does not cross the *x*-axis; instead the net heat of injection decreases monotonically to zero. This could be due in part to heterogeneity in the size of the injected vesicles. Vesicles of different radius might have slightly different chemical activities and, hence, show a break point at a different position in the titration curve. The observed titration curve would then represent a weighted average over the distribution of vesicle sizes. Another possible explanation for the discrepancy is that the relatively fast dissolution process is followed by a second, much slower process,

$$L_b + \nu D \overset{\text{fast}}{\rightleftharpoons} \Phi \overset{\text{slow}}{\rightleftharpoons} X \qquad (19)$$

where X could be, for example, an aggregated inclusion complex state or a second distinct lipid bilayer phase. In this scenario, the observed titration peaks would correspond to a fast relaxation toward a steady state, during which inclusion complexes would slowly convert to the final state X. If the fast step were endothermic and the second exothermic, the overall process could give a net injection heat that becomes negative after the end of the plateau part of the titration. But if the slow process produces a broad, shallow heat peak, it could disappear into the baseline, so only the initial fast process is measured by the calorimeter. Such a scenario is consistent with the pronounced broadening in the endothermic peaks seen in Figure 2.

Stoichiometry of the Inclusion Complex. In fitting to the titration data for POPC vesicles injected into mβCD solution, we assumed that all of the inclusion complexes formed had the same 1:ν stoichiometry. Although this assumption was motivated by a desire to reduce the number of fitting parameters, it is not crucial to our interpretation of the experimental results. Each of the incremental inclusion complexes in the stepwise mechanism shown in eq 10 has a concentration that is determined by the amount of free cyclodextrin present in the cell. In the experiments described here, the cyclodextrin was always present in a very large molar excess, and the extent of dilution by displacement of the injected aliquots was small, about 20% during the course of an entire titration. Therefore, the concentration of free mβCD in the calorimeter cell—and hence the distribution of different inclusion complexes—was approximately constant in these measurements. Furthermore, the concentration of each inclusion complex would have a break point at the same point in the titration. We can therefore regard the best-fit value of $\nu \doteq 4$ as an average for an ensemble of inclusion complexes.

In terms of molecular structure, a stoichiometry of $\nu = 4$ for POPC/mβCD inclusion complexes is consistent with the finding that dehydrated inclusion complexes of fatty acids containing 12−15 carbon atoms with native β-cyclodextrin tend to have a stoichiometry of 1:2 (*34*). POPC has two acyl chains having 16 and 18 carbon atoms (about 2 nm in length); for comparison, the height of the mβCD cavity is about 0.8 nm (*1*). These facts suggest that the acyl chains of POPC are splayed apart in the inclusion complex, with each included within two mβCD molecules (see below).

Equilibrium Constant and Enthalpy of Inclusion Complex Formation. The best-fit values of the molar heat of reaction and equilibrium constant for formation of the POPC/mβCD inclusion complex are $\Delta\bar{H}^{\circ}_{\Phi} \doteq 46$ kJ mol^{-1} and $K_{\Phi} \doteq 90$ M^{-3}. It is difficult to compare these values with those of inclusion complexes of cyclodextrins and other lipophiles because the bulk of published data is for complexes with a 1:1 stoichiometry. Furthermore, the overall formation reaction here involves transfer of a lipid molecule from a hydrophobic bilayer environment into the aqueous phase, whereas most studies of inclusion complex formation involve at least sparingly soluble guest molecules. However, the values that we obtained for the incremental addition of a

cyclodextrin molecule to a preexisting POPC/mβCD inclusion complex can be usefully compared with data for other complexes.

Of more than 400 β-cyclodextrin inclusion complexes described in the literature, the vast majority have values of $\Delta\bar{H}^\circ$ between −50 and 0 kJ mol^{-1} (*35*); the same is true of complexes with methylated β-cyclodextrins (*2*). Most reported binding constants are greater than 50 M^{-1}. These are in contrast to our values of $\Delta\bar{H}_i^\circ \doteq 15$ kJ mol^{-1} and $K_i \doteq 10$ M^{-1}. Our results show that, unlike nearly all previously known cyclodextrin inclusion complexes, the complexation of POPC and mβCD is weak and is driven exclusively by entropy. We shall not attempt to further explain the atypical thermodynamic parameters of POPC−mβCD interaction, except to note that the values of $\Delta\bar{H}_i^\circ$ and K_i cited here refer to complexation of a cyclodextrin molecule with a preexisting complex in the aqueous environment.

The energetics of transfer of POPC from an apolar bilayer environment into water, which do not contribute to the values of $\Delta\bar{H}_i^\circ$ and K_i, can be estimated by combining those parameters with $\Delta\bar{H}_1^\circ$ and K_1. To the extent that the attachment of a cyclodextrin molecule to aqueous POPC is equivalent for each of the four steps of eq 10, the dissolution reaction

$$L_b \rightleftarrows L_{aq} \tag{20}$$

is described by $\Delta\bar{H}^\circ = \Delta\bar{H}_1^\circ/\Delta\bar{H}_i^\circ \doteq -17$ kJ mol^{-1} and $K = K_1/K_i \doteq 8$ mM. This enthalpy change is in line with values for short hydrocarbon chains (*29*), but the equilibrium constant probably overestimates the actual solubility of POPC by several orders of magnitude. In light of all of the assumptions involved in obtaining these values, however, they seem fairly reasonable.

On the basis of the location of the boundary of POPC solubility in mβCD solution, there did not appear to be a significant difference between the equilibrium constant of inclusion complex formation for 30 nm sonicated vesicles, for 50 and 100 nm extruded vesicles, and for multilamellar vesicles (Figure 4). Variation in the enthalpy of inclusion complex formation for unilamellar vesicles of differing diameter, and between uni- and multilamellar vesicles, was within experimental error. The large uncertainty in these measurements arises in part from the need to subtract a large heat of dilution from a large integrated heat of injection, and efforts are under way to refine these measurements. We note that some variation in $\Delta\bar{H}_\Phi^\circ$ with vesicle size is to be expected because the enthalpy of the vesicle bilayer is a function of the radius of curvature (*36*).

The POPC/cyclodextrin titrations shown in Figure 6 indicate a pronounced temperature dependence for the complexation reaction. Studies of proteins have suggested that the transfer of an apolar surface of 1 nm^2 from a polar to a nonpolar environment contributes a heat capacity change of about −0.19 kJ mol^{-1} (*37*). Our calculated heat capacity change of $\Delta C_P^\circ = -1.0$ kJ mol^{-1} therefore would be consistent with a net transfer of about 5 nm^2 of hydrophobic surface from water into a nonpolar environment. For comparison, if we regard the cavity of mβCD as a cylinder of radius 0.3 nm and height 0.8 nm, its hydrophobic surface is about 1.5 nm^2, for a total of 6 nm^2 for the four cyclodextrin molecules in the complex. That is, the cyclodextrin molecules alone can account for all of the observed change in heat capacity for inclusion complex formation. This is reasonable if the hydrophobic POPC acyl chains are in nonpolar enviroments in both the bilayer and the inclusion complex.

Mechanism of Inclusion Complex Formation. There are three basic mechanisms that are consistent with the overall reaction in eq 1. One is the stepwise mechanism of eq 10, in which a single cyclodextrin molecule comes into contact with the lipid bilayer and extracts a phospholipid molecule to form a 1:1 complex, after which additional cyclodextrin molecules are attached, forming complexes of successively larger stoichiometry. As an alternative, two or more cyclodextrin molecules might associate to form an oligomer, which then extracts a lipid molecule from the bilayer. Finally, cyclodextrin, either individually or as an oligomer, could bind to a lipid monomer in aqueous solution. This last alternative can be ruled out because the spontaneous release of long-chain phospholipid monomers into solution takes place on a time scale of hours (*38*), which is far too slow to produce injection peaks that span only a few minutes. Although we cannot rule out oligomerization of mβCD in solution, measurements of the heat of mβCD dilution show no evidence for the presence of oligomers, nor do measurements of the surface pressure of mβCD monolayers (T. G. Anderson and G. Gerebtzoff, unpublished results). As a result, we favor the stepwise mechanism of eq 10. A similar mechanism was proposed by Debouzy for the interaction of αCD with phospholipid vesicles (*19*). It is known from DSC measurements that some forms of βCD interact with intact phospholipid bilayers (*16*). This interaction is likely to be transient, however, as demonstrated by the lack of binding of radiolabeled βCD to erythrocyte membranes (*13*). The need for direct contact between cyclodextrin and the vesicle surface may explain why hpβCD, which is not a surface-active molecule, does not rapidly form inclusion complexes with POPC, whereas the highly surface-active mβCD does.

Since the formation of POPC/mβCD inclusion complexes is reversible, mβCD likely can act as a catalyst for the transfer of POPC monomers from one vesicle to another and between vesicles and an aqueous solution. This could accelerate the Ostwald ripening-like process of growth of larger vesicles at the expense of smaller, less-stable ones that is ordinarily very slow (*39*).

The calorimetric results presented here provide no details about the structure of POPC/mβCD inclusion complexes, apart from the range of stoichiometries. On the basis of the observed $n = 4$ stoichiometry and the relative dimensions of the molecules noted earlier, we tentatively suggest that each acyl chain of the POPC molecule is separately complexed by 1−2 mβCD molecules. This type of structure has been proposed for inclusion complexes of phosphatidylinositol and αCD on the basis of nuclear magnetic resonance data (*18*). Alternative structures are possible, however. For example, the acyl chains might be "sandwiched" between pairs of cyclodextrin molecules, rather than penetrating their cavities, or the two acyl chains might be aligned in parallel through the cavities of four cyclodextrins. Although there is room in the βCD cavity for two carbon chains side by side (*40*), we consider that possibility unfavorable on steric grounds.

Implications for Other Studies. The high cooperativity observed here for formation of POPC/mβCD inclusion

complexes translates into a high sensitivity to the concentration of the cyclodextrin. The technique of ITC is particularly suited to take advantage of this because the injectant is diluted by a factor of about 100 upon injection into the calorimeter cell. Injection of preformed inclusion complexes would result in the release of phospholipid monomers, which would partition into any suitable hydrophobic environment that is present.

Methyl-β-cyclodextrin is a convenient and inexpensive sequestering agent for a wide variety of hydrophobic molecules that are of biomedical interest. The results presented here show that at high concentrations mβCD can solubilize phospholipid membranes, which may be undesirable. This solubilization can be avoided by working with mβCD concentrations below ~15 mM, which is adequate for many applications.

ACKNOWLEDGMENT

We thank Katherine Oaks and Heiko Heerklotz for helpful comments on this manuscript.

APPENDIX

Calculation of Titration Curves. For an injection of an aliquot with a volume of ΔV_{inj} into the calorimeter cell, the measured heat of injection is

$$Q_{inj} = Q_{disp} + Q_{mix} \quad (21)$$

where Q_{disp} is the heat associated with the physical displacement of the volume element ΔV_{inj} that mainly arises from a small difference between the temperatures of the syringe and cell and Q_{mix} is the heat of mixing of the injected aliquot with the contents of the cell. Q_{disp} is measured by injecting buffer into buffer and is typically of the order of 1−2 μJ/μL injected. The heat of mixing is

$$Q_{mix} = H_{cell}(\text{final}) - H_{cell}(\text{initial}) \quad (22)$$

The final enthalpy of the cell is a function of composition, $H(c_f)$, where c_f is the final concentration of injectant in the cell. The initial enthalpy of the cell *after the volume displacement but before mixing* is

$$H_{cell}(\text{initial}) = \left(\frac{V_{cell} - \Delta V_{inj}}{V_{cell}}\right)H(c_i) + \left(\frac{\Delta V_{inj}}{V_{cell}}\right)H(c_{syr}) \quad (23)$$

where c_i is the initial concentration of injectant in the cell and $H(c_{syr})$ is the enthalpy of the cell if its *entire* composition were equal to that of the syringe; if the heat of dilution is ignored, the latter term can usually be set equal to zero. Combining eqs 21−23 gives, after rearrangement of terms,

$$Q_{inj} = Q_{disp} + H(c_f) - H(c_i) + \frac{\Delta V_{inj}}{V_{cell}}(H(c_i) - H(c_{syr})) \quad (24)$$

To account for the fact that the injection is not instantaneous, ΔV_{inj} can be replaced by dV in eq 24; integration over the injected volume then gives the exact expression

$$Q_{inj} = Q_{disp} + H(c_f) - H(c_i) + \frac{1}{V_{cell}}\int_{V_i}^{V_f}(H(c_V) - H(c_{syr}))\,dV \quad (25)$$

Since the concentration of injectant generally does not change much during the course of an injection, the integrand in eq 25 can be approximated by $H(c_{1/2})$, the enthalpy of the cell at a composition corresponding to the midpoint of the injection.

The heat of injection per mole of injectant is found by dividing Q_{inj} by the amount injected, $\Delta n_{inj} = c_{syr}\Delta V_{inj}$.

The calculated titration curves shown in Figure 7 were generated using eq 25 with the enthalpy function

$$H(c_L^0) = \Delta\bar{H}_\Phi^\circ V_{cell} c_\Phi \quad (26)$$

where the concentration of the inclusion complex is found by solving eq 4.

REFERENCES

1. Szejtli, J. (1998) Introduction and General Overview of Cyclodextrin Chemistry, *Chem. Rev. 98*, 1743−1753.
2. Rekharsky, M. V., and Inoue, Y. (1998) Complexation Thermodynamics of Cyclodextrins, *Chem. Rev. 98*, 1875−1917.
3. Uekama, K., Hirayama, F., and Irie, T. (1998) Cyclodextrin Drug Carrier Systems, *Chem. Rev. 98*, 2045−2076.
4. De Caprio, J., Yun, J., and Javitt, N. B. (1992) Bile acid and sterol solubilization in 2-hydroxypropyl-β-cyclodextrin, *J. Lipid Res. 33*, 441−443.
5. Kilsdonk, E. P. C., Yancey, P. G., Stoudt, G. W., Bangerter, F. W., Johnson, W. J., Phillips, M. C., and Rothblat, G. H. (1995) Cellular Cholesterol Efflux Mediated by Cyclodextrins, *J. Biol. Chem. 270*, 17250−17256.
6. Leventis, R., and Silvius, J. R. (2001) Use of Cyclodextrins to Monitor Transbilayer Movement and Differential Lipid Affinities of Cholesterol, *Biophys. J. 81*, 2257−2267.
7. Ohvo, H., and Slotte, J. P. (1996) Cyclodextrin-Mediated Removal of Sterols from Monolayers: Effects of Sterol Structure and Phospholipids on Desorption Rate, *Biochemistry 35*, 8018−8024.
8. Radhakrishnan, A., and McConnell, H. M. (2000) Chemical Activity of Cholesterol in Membranes, *Biochemistry 39*, 8119−8124.
9. Niu, S.-L., and Litman, B. J. (2002) Determination of Membrane Cholesterol Partition Coefficient Using a Lipid Vesicle-Cyclodextrin Binary System: Effect of Phospholipid Acyl Chain Unsaturation and Headgroup Composition, *Biophys. J. 83*, 3408−3415.
10. Yancey, P. G., Rodrigueza, W. V., Kilsdonk, E. P. C., Stoudt, G. W., Johnson, W. J., Phillips, M. C., and Rothblatt, G. H. (1996) Cellular Cholesterol Efflux Mediated by Cyclodextrins, *J. Biol. Chem. 271*, 16026−16034.
11. Podar, K., Tai, Y.-T., Cole, C. E., Hideshima, T., Sattler, M., Hamblin, A., Mitsiades, N., Schlossman, R. L., Davies, F. E., Morgan, G. J., Munshi, N. C., Chauhan, D., and Anderson, K. C. (2003) Essential Role of Caveolae in Interleukin-6- and Insulin-like Growth Factor I-triggered Akt-1-mediated Survival of Multiple Myeloma Cells, *J. Biol. Chem. 278*, 5794−5801.
12. Choi, Y.-H., Yang, C.-H., Kim, H.-W., and Jung, S. (2001) Molecular Modeling Studies of the β-Cyclodextrin in Monomer and Dimer Form as Hosts for the Complexation of Cholesterol, *J. Inclusion Phenom. Macrocyclic Chem. 39*, 71−76.
13. Ohtani, Y., Irie, T., Uekama, K., Fukunaga, K., and Pitha, J. (1989) Differential effects of α-, β-, and γ-cyclodextrins on human erythrocytes, *Eur. J. Biochem. 186*, 17−22.
14. Legendre, J. Y., Rault, I., Petit, A., Luijten, W., Demuynck, I., Horvath, S., Ginot, Y. M., and Cuine, A. (1995) Effects of β-cyclodextrins on skin: implications for the transdermal delivery of piribedil and a novel cognition enhancing-drug, S-9977, *Eur. J. Pharm. Sci. 3*, 311−322.
15. Niu, S.-L., Mitchell, D. C., and Litman, B. J. (2002) Manipulation of Cholesterol Levels in Rod Disk Membranes by Methyl-β-Cyclodextrin, *J. Biol. Chem. 277*, 20139−20145.

16. Puglisi, G., Fresta, M., and Ventura, C. A. (1996) Interaction of Natural and Modified β-Cyclodextrins with a Biological Membrane Model of Dipalmitoylphosphatidylcholine, *J. Colloid Interface Sci. 180*, 542−547.
17. Nishijo, J., and Mizuno, H. (1998) Interactions of Cyclodextrins with DPPC Liposomes. Differential Scanning Calorimetry Studies, *Chem. Pharm. Bull. 46*, 120−124.
18. Fauvelle, F., Debouzy, J. C., Crouzy, S., Göschl, M., and Chapron, Y. (1997) Mechanism of α-Cyclodextrin-Induced Hemolysis. 1. The Two-Step Extraction of Phosphatidylinositol from the Membrane, *J. Pharm. Sci. 86*, 935−943.
19. Debouzy, J. C., Fauvelle, F., Crouzy, S., Girault, L., Chapron, Y., Göschl, M., and Gadelle, A. (1998) Mechanism of α-Cyclodextrin Induced Hemolysis. 2. A Study of the Factors Controlling the Association with Serine-, Ethanolamine-, and Choline-Phospholipids, *J. Pharm. Sci. 87*, 59−66.
20. Nishijo, J., Shiota, S., Mazima, K., Inoue, Y., Mizuno, H., and Yoshida, J. (2000) Interactions of Cyclodextrins with Dipalmitoyl, Distearoyl, and Dimyristoyl Phosphatidyl Choline Liposomes. A Study by Leakage of Carboxyfluorescein in Inner Aqueous Phase of Unilamellar Liposomes, *Chem. Pharm. Bull. 48*, 48−52.
21. Tanhuanpää, K., and Somerharju, P. (1999) γ-Cyclodextrins Greatly Enhance Translocation of Hydrophobic Fluorescent Phospholipids from Vesicles to Cells in Culture, *J. Biol. Chem. 274*, 35359−35366.
22. Tanhuanpää, K., Cheng, K. H., Anttonen, K., Virtanen, J. A., and Somerharju, P. (2001) Characteristics of Pyrene Phospholipid/γ-Cyclodextrin Complex, *Biophys. J. 81*, 1501−1510.
23. Almog, S., Litman, B. J., Wimley, W., Cohen, J., Wachtel, E. J., Barenholz, Y., Ben-Shaul, A., and Lichtenberg, D. (1990) States of Aggregation and Phase Transformations in Mixtures of Phosphatidylcholine and Octyl Glucoside, *Biochemistry 29*, 4582−4592.
24. Wiseman, T., Williston, S., Brandts, J. F., and Lin, L. N. (1989) Rapid measurement of binding constants and heats of binding using a new titration calorimeter, *Anal. Biochem. 179*, 131−137.
25. MacDonald, R. C., MacDonald, R. I., Menco, B. P., Takeshita, K., Subbarao, N. K., and Hu, L. R. (1991) Small-volume extrusion apparatus for preparation of large, unilamellar vesicles, *Biochim. Biophys. Acta 1061*, 297−303.
26. Israelachvili, J. (1992) *Intermolecular & Surface Forces*, 2nd ed., p 357, Academic Press, New York.
27. Tanford, C. (1980) *The Hydrophobic Effect: Formation of Micelles and Biological Membranes*, 2nd ed., Wiley, New York.
28. Connors, K. A. (1997) The Stability of Cyclodextrin Complexes in Solution, *Chem. Rev. 97*, 1325−1357.
29. Widom, B., Bhimalapuram, P., and Koga, K. (2003) The hydrophobic effect, *Phys. Chem. Chem. Phys. 5*, 3085−3093.
30. Wenk, M. R., and Seelig, J. (1997) Vesicle−Micelle Transformation of Phosphatidylcholine/Octyl-β-D-glucopyranoside Mixtures As Detected with Titration Calorimetry, *J. Phys. Chem. B 101*, 5224−5231.
31. Heerklotz, H., and Seelig, J. (2000) Titration calorimetry of surfactant-membrane partitioning and membrane solubilization, *Biochim. Biophys. Acta 1508*, 69−85.
32. Garidel, P., Hildebrand, A., Neubert, R., and Blume, A. (2000) Thermodynamic Characterization of Bile Salt Aggregation as a Function of Temperature and Ionic Strength Using Isothermal Titration Calorimetry, *Langmuir 16*, 5267−5275.
33. Tan, A., Ziegler, A., Steinbauer, B., and Seelig, J. (2002) Thermodynamics of Sodium Dodecyl Sulfate Partitioning into Lipid Membranes, *Biophys. J. 83*, 1547−1556.
34. Schlenk, H., and Sand, D. M. (1961) The Association of α- and β-Cyclodextrins with Organic Acids, *J. Am. Chem. Soc. 83*, 2312−2320.
35. Burnette, R. R., and Connors, K. A. (2000) Statistical Properties of Thermodynamic Quantities for Cyclodextrin Complex Formation, *J. Pharm. Sci. 89*, 1389−1394.
36. Cevc, G., and Marsh, D. (1987) *Phospholipid Bilayers, Physical Principles and Models*, Wiley, New York.
37. Baker, B. M., and Murphy, K. P. (1998) Prediction of Binding Energetics from Structure Using Empirical Parametrization, *Methods Enzymol. 295*, 294−315.
38. Nichols, J. W., and Pagano, R. E. (1982) Use of Resonance Energy Transfer to Study the Kinetics of Amphiphile Transfer between Vesicles, *Biochemistry 21*, 1720−1726.
39. Martin, F. J., and MacDonald, R. C. (1976) Phospholipid Exchange between Bilayer Membrane Vesicles, *Biochemistry 15*, 321−327.
40. Li, G., and McGown, L. B. (1994) Molecular Nanotube Aggregates of β- and γ-Cyclodextrins Linked by Diphenylhexatrienes, *Science 264*, 249−251.

BI0358869